Catalytic graphitization of wood-based carbons with alumina by pulse current heating

Hata, T.; Ishimaru, K.; Fujisawa, M.; Bronsveld, P; Vystavel, T.; De Hosson, J.; Kikuchi, H; Nishizawa, T.; Imamura, Y.

Published in:
Fullerenes Nanotubes and Carbon Nanostructures

DOI:
10.1081/FST-200039431

Publication date:
2005

Fullerenes, Nanotubes, and Carbon Nanostructures, 13: 435–445, 2005

ISSN 1536-383X print/1536-4046 online
DOI: 10.1081/FST-200039431

Catalytic Graphitization of Wood-Based Carbons with Alumina by Pulse Current Heating

T. Hata, K. Ishimaru, and M. Fujisawa
Research Institute for Sustainable Humanosphere, Kyoto University, Uji, Kyoto, Japan

P. Bronsveld, T. Vystavel, and J. De Hosson
Department of Applied Physics, Materials Science Centre, University of Groningen, The Netherlands

H. Kikuchi
S. S. Alloy, Hiroshima, Japan

T. Nishizawa and Y. Imamura
NanoCarbon Research Institute, Chosei, Chiba, Japan

Abstract: Japanese cedar was preheated at 500°C and subsequently mixed with 40 μm Al_2O_3 particles. A pulse current heating method was used for a 5-min carbonization step under a pressure of 50 MPa in order to promote the graphitization at temperatures between 2000 and 2200°C. The samples were analyzed in an analytical transmission electron microscope equipped with a GATAN Imaging Filter, in a high resolution transmission electron microscope and in a scanning electron microscope. Transformation into well-ordered graphite could be enforced by the intermediate reaction of Al_2O_3 and carbon to plate-like Al_4C_3. This latter compound dissociates under the proper CO pressure and temperature into Al vapor and solid graphite. The addition of Al_2O_3 and the pressurized heating device improve the graphitization in comparison with the effect of temperature alone. The electron microscopic observations are supported by XPS and XRD spectra.

Keywords: Charcoal, catalytic graphitization, carbonization, electron

Address correspondence to T. Hata, Research Institute for Sustainable Humanosphere, Kyoto University, Uji, Kyoto 611-0011, Japan. E-mail: hata@rish.kyoto-u.ac.jp

INTRODUCTION

The process of catalytic graphitization of ungraphitized carbon has been extensively studied (1–4). In the presence of catalysts such as Fe, Co, and Ni, the graphitization accelerates and runs at a lower temperature, in the case of solid-phase graphitization even below 1500°C (5). However, the effect of a catalyst is not as obvious and the contamination by the catalyst itself should be avoided. In the present paper, results are reported on the graphitization of biomass carbon influenced by the addition of aluminum oxide powder. During heating, a compressed powder mix of biomass carbon and Al_2O_3, graphitization develops by formation and dissociation of Al_4C_3. A comparison is made between the catalytic graphitization in biomass carbon mixed with alumina powder and graphitization in pure biomass carbon without alumina. Both types were carbonized at temperatures up to 2200°C during 5 min under an argon pressure of 50 MPa. This paper is the second in a series about wood charcoal where the pressurized heating device improve the graphitization in comparison with the effect of temperature alone. Earlier, we reported on graphitization of wood charcoal, liquid mixed with Al-triisopropoxide using High Resolution Electron Microscopy in combination with x-ray powder diffraction (6). In this second paper XPS data were also collected in order to identify the graphite (7–10).

EXPERIMENTAL

Sugi (*Cryptomeria japonica*) powder was preheated in an electric furnace up to 500°C and kept constant for 60 min under an argon atmosphere. Subsequently, the preheated samples were crunched and mixed with alumina particles of 40 μm in size. A pulse current heating apparatus (Plasman, S.S. Alloy, Hiroshima) was used to heat the powder mix. Electric pulses and pressure were directly applied to the powder mix inside the die (Fig. 1). The weight percentage of alumina was 0, 10, 20, and 30% based on the weight of dry wood charcoal. The heat treatment was at 2000 to 2200°C for 5 min under 50 MPa.

The XPS spectra were collected on a AXIS-HS (Shimadzu/KRATOS) machine using an MgKα (1253.6 eV) x-ray source operating at 150 W in a vacuum of 2.5×10^{-8} Torr. High-resolution scans of C_{1s} were performed with the pass energy adjusted to 40 eV. The curve fitting of the XPS spectra was carried out using a nonlinear least squares curve-fitting algorithm with a Gaussian/Lorentzian product function. The Gaussian/Lorentzian mix was taken as 0.5, except for the "graphitic" carbon peak, for which 0.84 was used with an exponential tail. The C_{1s} binding energy of the graphite peak was taken as 284.3 eV for calibration purposes (7). An x-ray diffraction device (RINT-ultra X18) was used to determine the crystal structure.

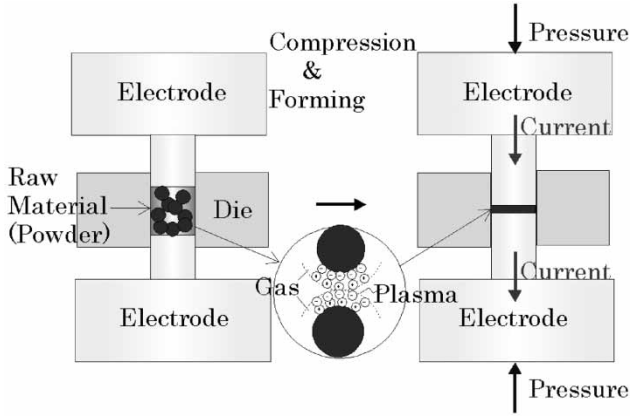

Figure 1. Pulse current heating apparatus, in which an electric pulse was directly applied to the power of wood charcoal mixed with Al_2O_3.

The samples were analyzed in a JEOL 2010 F analytical TEM operated at 200 kV and fitted with a GATAN post column energy filter, in a JEOL 4000 EX/II high-resolution TEM operated at 400 kV and in a FEI XL 30S SEM.

RESULTS AND DISCUSSION

Photoelectron Spectroscopy and X-ray Diffraction

The samples treated with alumina showed much narrower peaks than those consisting of pure wood charcoal and the peak centers were shifted to lower binding energy, as the alumina concentration became higher. A special effort was made to take care of contributions of graphite as well as of the non-graphite contributions. In Table 1 the result of that exercise is reproduced with the assignments and positions of two peaks, the first peak being due to graphite and the second peak covering the non-graphite contributions. We took the overlapping peak, C1s, of natural graphite as the deconvoluted peak, C1, because of the long tailing peak of the samples showing the shake-up peak belonging to that of graphite.

A nice similarity was found between the model peak C1s from graphite and the C1 peak from our sample. After applying the model of the overlapping peak of natural graphite, we added another deconvoluted peak, to which we set the peak position free in order to estimate the difference between the peak from the sample and that from graphite. After deconvolution, the area of the C2 peak was zero in the sample at 2200°C treated with Al, and 26.6 at.% at 2000°C without Al, of which the C2 peak position was 285.2.

Table 1. Analysis of the C_{1s} peak for wood charcoal with different concentrations of Al_2O_3 heat-treated for 5 min at the indicated temperatures. C_1: Graphite; C_2: Nongraphite contributions

		Area of the C_{1s} peaks (at%)		
Temp (°C)	AL (%)	C_1* (284.3)	C_2 (285.2)	C_{1s}** FWHM
2000	0	73.4	26.6	1.61
2200	0	100.0	0.0	1.11
2200	10	100.0	0.0	1.05
2200	20	100.0	0.0	1.07
2200	30	100.0	0.0	1.05

Note: *C_{1s} peak with FWHM of 1.09, for natural graphite powder supplied by Nacalai Tesque Ltd.
**Overlapping peaks.

The full width at half maximum (FWHM) of the C1s peak has been listed in Table 1. Judging from these results and in combination with HREM images it became clear that the higher the degree of graphitization the narrower this peak is and the smaller the contribution of C2. The FWHM decreases with increasing temperature and increasing concentration of alumina. The spectra and list of half widths show that the degree of graphitization has been maximized (7) in the sample at 2200°C treated with Al.

In Fig. 2 X-ray powder scans are reproduced for samples with 0, 10, 20, and 30 wt.% Al heated at 2000 and 2200°C for 5 min. The Al_2O_3 peaks could just be observed in the 20 and 30 wt.% Al samples. The carbon peaks correspond to the graphite phase: [0 0 2], [1 0 0], [1 0 1], [0 0 4], and [1 1 0]. The detection of such carbon peaks can be considered as proof that mixing of charcoal with alumina powder combined with the heat treatment by pulse current heating accelerates the process from biomass to graphitic structure.

Electron Microscopy

In Fig. 3a–3c images are depicted of the catalytic activity in the wood carbon sample with 10% alumina at 2200°C. In Fig. 3a thin plate-like structures are observed which could be found easily in samples with 30% Al_2O_3, but less so for those with 10%. EDS analysis proved the 10% samples to be almost free of aluminum after 5 min at 2200°C and this was not the case for the 30% samples. The inclusions in Fig. 3b were identified by EDS as Al_2O_3 particles still in the process of being transformed from oxide to carbide. They are surrounded by a microfibrillar structure, which are speculated to be aggregated carbonized

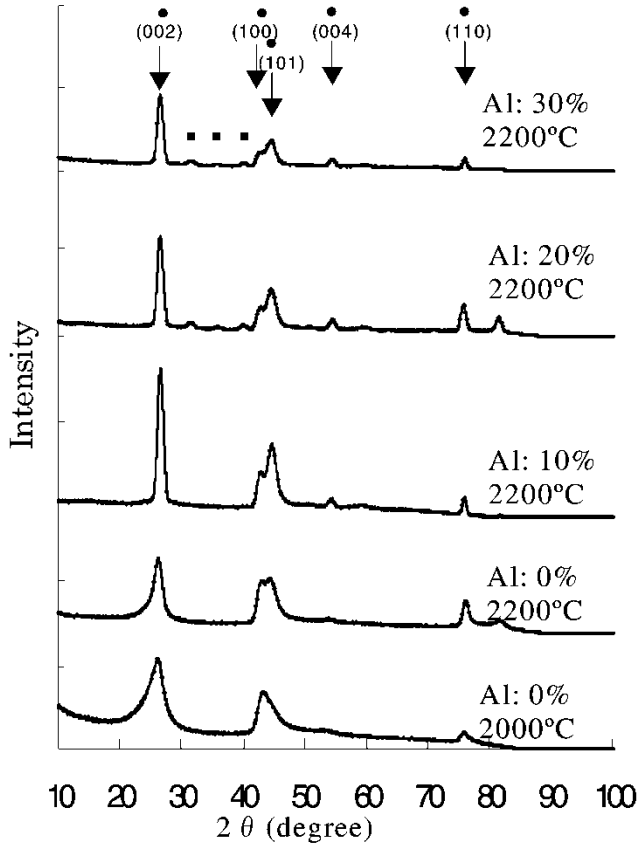

Figure 2. X-ray powder-scans of specimens heated at 2000 and 2200°C for 0, 10, 20, and 30 wt.% Al. (●) C; (■) Al_2O_3.

micro fibrils of which alignment and size are derived from the microfibrils in the original wood. The close contact at the interface between the Al_2O_3 and the microfibrillar structure suggest that the wetting problem above 1800°C of aluminum with carbon is circumvented by this method of pulse current heating under pressure.

In Fig. 3c an HREM image of a specimen with 10% Al_2O_3 at 2200°C shows a transition from an amorphous to a curved graphitic layer structure with 0.34 nm per single fringe distance. This type of structure was also observed in samples without alumina and could still be caused solely by the high temperature.

The TEM image in Fig. 4 shows a single crystallized slab with its diffraction pattern as insert. It clearly shows the typical 0.416 nm interplanar spacing for the [0 0 0 6] planes in Al_4C_3 (trigonal crystal structure, R-3m with

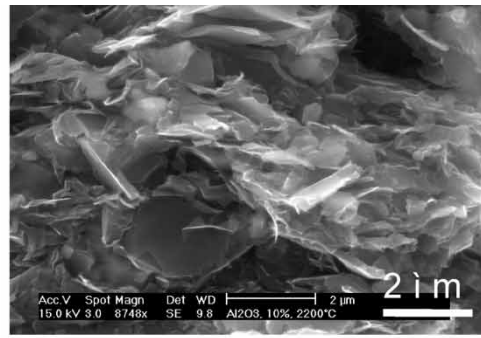

(a) Micron sized Al_4C_3 plates are visible.

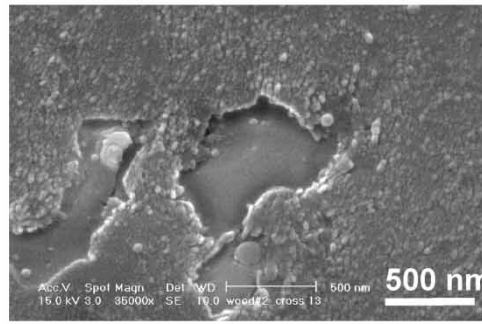

(b) Transformation from Al_2O_3 to Al_4C_3 still underway.

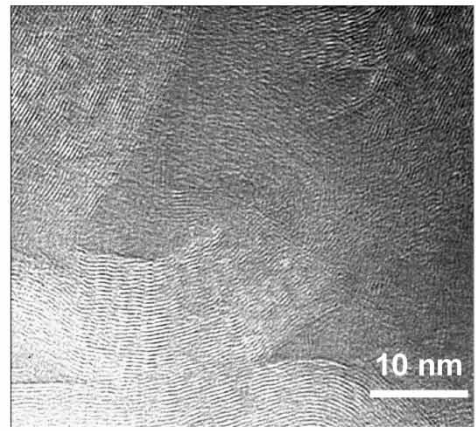

(c) Graphite fringe distance of 0.34 nm.

Figure 3. SEM and TEM images of charcoal with 10% Al_2O_3; 5 min at 2200°C; 50 MPa.

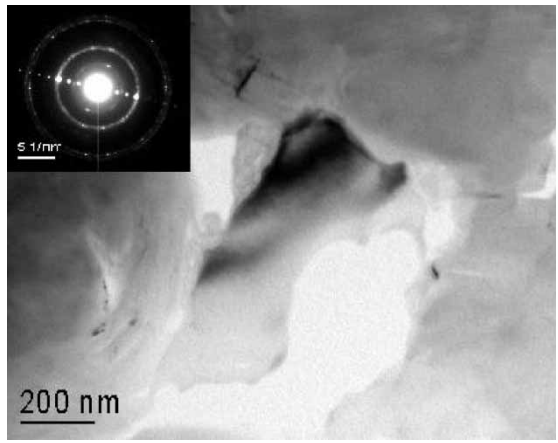

Figure 4. Graphitized structure of charcoal with 30% Al_2O_3; 5 min at 2200°C. SADPof the Al_4C_3 plate is enclosed.

$a_0 = 0.333$ nm and $c_0 = 2.499$ nm). The basal planes in the Al_4C_3 plates are parallel to the long sides of the plates, indicating that the main growing direction is along the [0 0 0 1] planes. A porous reaction layer could be observed all around the Al_4C_3 plate. CO formation during the reaction between Al_2O_3 and C must be the reason for this porous structure. This separate patch was mapped by EFTEM as is shown in Fig. 5. A decreasing

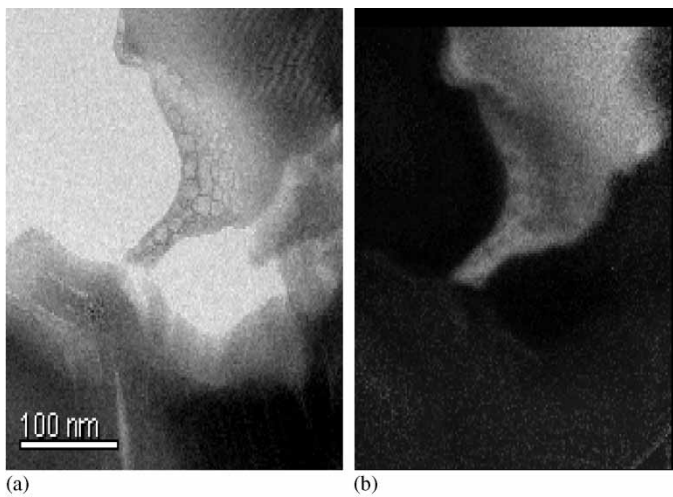

Figure 5. Energy-filtered TEM: (a) Zero loss image; (b) elemental map (Green: Al, Red: O, Blue: (c) of reaction area of original Al_2O_3 particle. Charcoal with 30% Al_2O_3; 5 min at 2200°C.

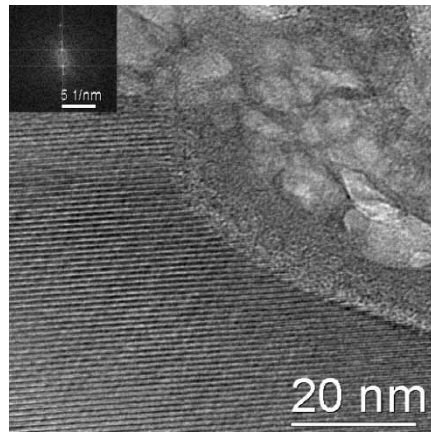

Figure 6. Details of the transformation of Al_2O_3 (upper right) into Al_4C_3 (lower left). Charcoal with 30% Al_2O_3; 5 min at 2200°C.

amount of oxygen is observed going from the center of the image towards the upper right hand side. Obviously, it is a particle in transition from oxide to carbide, originally occupying the central area, of which the centerpiece was removed by thinning during sample preparation. A detailed image is depicted in Fig. 6 with as most dominant part the Al_4C_3 phase in the lower left hand corner. A porous interface layer where the transformation into the plate like Al_4C_3 occurred while the gas was being formed is clearly shown in the upper right hand corner.

In Fig. 7 proof is given of the Al_4C_3 being decomposing even further into solidgraphite. The dark areas in the graphite structure are due to severe bending of the graphite layers diffracting away the electron beam. It is obvious from the right hand side of the image that the graphite structure is bending away upwards, caused by the location of the original Al_2O_3 particle. Sometimes kink bands were observed in the graphite layers. The aluminum vapor could be traced back as a coating on the inner wall of the heat shield in the furnace.

One can conclude that mixing charcoal with alumina powder accelerated the process from biomass to graphite. The notoriously poor ability of biomass to transform into large areas of well-ordered graphite can be surpassed by making use of the intermediate reaction between Al_2O_3 and carbon forming plate-like Al_4C_3.

DISCUSSION

According to Yu et al.[13] the process of graphitization develops catalytically by formation and dissociation of plate-like Al_4C_3 from alumina and carbon.

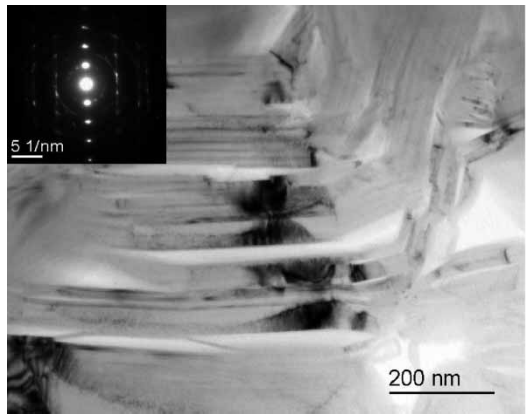

Figure 7. Graphitized structure of charcoal with 30% Al_2O_3; 5 min at 2200°C.

As the Al_4C_3 phase is thermodynamically unstable above 1900°C, Al(g) and C(s) occur in the Al-C-O system following the equations:

$$2Al_2O_3 + 9C(s) \longrightarrow Al_4C_3(s) + 6CO(g) \quad (1)$$

$$Al_4C_3(s) \longrightarrow 4Al(g) + 3C\ gr(s) \quad (2)$$

The Al_4C_3 is a suitable equilibrium phase at relatively high temperature and low CO, (g) pressure and indeed Al_4C_3 plate-like crystallites were observed in the sample at 2200°C with 30% Al_2O_3.

One should realize that the Al_2O_3 phase is giving way to the Al_4C_3 phase under suitable temperature and CO pressure. Establishing the equilibrium condition written explicitly in Eqs. (1) and (2) determines how much graphite will be formed. One has to bring the carbon particles and the alumina particles in close contact to achieve the transformation into the plate-like Al_4C_3 while CO is being formed. The dissociation of Al_4C_3 under the proper CO pressure into Al vapour and solid graphite obviously did occur in the specimen.

The high temperature-high pressure heating step may be instrumental in achieving the right partial pressure of CO in Eq. (1). Removal of the Al-vapour towards the outside of the die forces the chemical reaction of Eq. (2) towards the right hand side. Lihrmann et al. (12) emphasises the point that the intermediate phases of Al_4O_4C and Al_2OC are being formed but not the Al_4C_3. However, we have proof from the diffraction pattern in Fig. 6 that Al_4C_3 has been formed. HREM, EDS, and EELS examinations of the interfacial reaction layers of the Al_2O_3/C have shown the specific features of the catalytic reaction process.

CONCLUSION

Mixing of biomass carbon with alumina powder accelerates the process of graphitization. Its notoriously poor ability to transform into large areas of well-ordered graphite can be surpassed by introducing the intermediate reaction between Al_2O_3 and carbon forming plate-like Al_4C_3. The dissociation of Al_4C_3 under the proper CO pressure into Al vapor and solid graphite is confirmed by EFTEM. XPS-data confirm the ultimate graphite formation.

ACKNOWLEDGMENTS

The authors are grateful to Henk Bron and Uko Nieborg, for assistance with sample preparation and operation of the microscopes. This research was carried out with support from Grant-in-Aid for Scientific Research (13460078) from the Ministry of Education, Science, and Culture of Japan.

REFERENCES

1. Krivoruchko, O.P., Maksimova, N.I., Zaikovskii, V.I., and Salonov, A.N. (2000) Study of multiwalled graphite nanotubes and filaments formation from carbonized products of polyvinyl alcohol via catalytic graphitization at 600–800°C in nitrogen atmosphere. *Carbon*, 38: 1075–1082.
2. Oya, A., Yamashita, R., and Otani, S. (1978) Catalytic graphitization of charcoal by gaseous species formed from calcium. *High Temp.–High Pres.*, 10: 521–526.
3. Oya, A. and Marsh, H. (1982) Review phenomena of catalytic graphitization. *J. Mater. Sci.*, 17: 309–322.
4. Moreno, J.M.C., Swamy, S.S., Fujino, T., and Yoshimura, M. (2000) Carbon nanocells and nanotubes grown in hydrothermal fluids. *Chem. Phys. Lett.*, 329: 317–322.
5. Dhakate, S.R., Mathur, R.B., and Bahl, O.P. (1997) Catalytic effect of iron oxide on carbon/carbon composites during graphitisation. *Carbon*, 35: 1753–1756.
6. Hata, T., Nishimiya, K., Bronsveld, P., Vystavel, T., DeHosson, J., Kikuchi, H., and Imamura, Y. (2002) Electron microscopic study on catalytic carbonization of biomass carbon I carbonisation of wood charcoal at high temperature by Al-triisopropoxide. *Mol. Crystals Liq. Crys.*, 386: 33–38.
7. Darmstadt, H., Roy, C., and Kaliaguine, S. (1994) ESCA characterization of commercial carbon blacks and of carbon blacks from vacuum pyrolysis of used tires. *Carbon*, 32: 1399–1406.
8. Petukhov, M.N. and Dementjev, A.P. (1997) The development of C KVV X-ray-excited Auger spectroscopy for estimation of the $sp^2:sp^3$ ratio in DLC films. *J. Chem. Vapour Depos.*, 5: 230–236.
9. Ponsonnet, L., Donnet, C., Varlot, K., Martin, J.M., Grill, A., and Patel, V. (1998) EELS analysis of hydrogenated diamond-like carbon films. *Thin Solid Films*, 319: 97–100.

10. Redlich, P.H., Banhart, F., Lyutovich, Y., and Ajayan, P.M. (1998) EELS study of the irradiation-induced compression of carbon onions and their transformation to diamond. *Carbon*, 36: 561–563.
11. Yu, J.K., Ueno, S., Li, H.X., and Hiragushi, K. (1999) Improvement of graphitisation of isotropic carbon by Al_2O_3 formed from aluminium chelate compound. *J. Eur. Cer. Soc.*, 19: 2843–2848.
12. Lihrmann, J.-M., Tirlocq, J., Descamps, P., and Cambier, F. (1999) Thermodynamics of the Al-C-O system and properties of SiC-AlN-Al_2OC composites. *J. Eur. Cer. Soc.*, 19: 2781–2787.